



Cone-beam CT measurements of distal tibio-fibular syndesmosis in asymptomatic uninjured ankles: does weight-bearing matter?

Delaram Shakoor¹ · Greg M. Osgood² · Michael Brehler³ · Wojciech B. Zbijewski³ · Cesar de Cesar Netto⁴ · Babar Shafiq² · Jakrapong Orapin⁴ · Gaurav K. Thawait¹ · Lew C. Shon⁴ · Shadpour Demehri¹

Received: 28 June 2018 / Revised: 31 August 2018 / Accepted: 9 September 2018 / Published online: 21 September 2018
© ISS 2018

Abstract

Objective To evaluate the influence of weight-bearing (WB) load in standard axial ankle syndesmotomic measurements using cone beam CT (CBCT) examination of asymptomatic uninjured ankles.

Materials and methods In this IRB approved, prospective study, patients with previous unilateral ankle fractures were recruited. We simultaneously scanned the injured ankles and asymptomatic contralateral ankles of 27 patients in both WB and NWB modes. For this study, only asymptomatic contralateral ankles with normal plain radiographs were included. Twelve standardized syndesmosis measurements at two axial planes (10 mm above the tibial plafond and 5 mm below the talar dome) were obtained by two expert readers using a custom CBCT viewer with the capability for geometric measurements between user-identified anatomical landmarks. Inter-reader reliability between two readers was obtained using the intra-class correlation coefficient (ICC). We compared the WB and NWB measurements using paired *t* test.

Results Significant agreement was observed between two readers for both WB and NWB measurements ($p < 0.05$). ICC values for WB and NWB measurements had a range of 50–95 and 31–71 respectively. Mean values of the medial clear space on WB images (1.75, 95% confidence interval [95% CI]: 1.6, 1.9) were significantly lower than on NWB images (2.05, 95% CI: 1.8, 2.2) measurements ($p < 0.001$). There was no significant difference between the remaining WB and NWB measurements.

Conclusion Measurements obtained from WB images are reliable. Except for the medial clear space, no significant difference in syndesmotomic measurements were observed during the WB mode of CBCT acquisition, implying that the tibio-fibular relationship remains unchanged when the physiological axial weight-bearing load is applied.

Keywords Syndesmosis · Weight-bearing · Normal ankles · Cone-beam CT · Medial clear space

Introduction

Following ankle trauma, accurate assessment of syndesmotomic injuries is extremely important [1], because undiagnosed

injuries could lead to ongoing instability and long-term complications such as osteoarthritis [2–5]. In contrast, syndesmotomic injuries are often associated with nonspecific clinical findings, thus mandating additional imaging studies, preferably in weight-bearing (WB) mode, to unmask occult diastasis [5–7]. However, ankle radiographs have been shown to be unreliable, mainly because of the variability of ankle positioning using two-dimensional (2D) radiographs for such measurements [8–10]. In addition, traditional radiographic measurements, including the tibio-fibular clear space (TFCS) and the tibio-fibular overlap (TFO), are poorly defined and reported to be inaccurate for evaluating the distal tibio-fibular relationship [5, 9].

Recent reports have suggested that computed tomography (CT) can evaluate distal tibio-fibular configuration accurately and reliably [5, 8, 11, 12]. The anatomy of the distal tibio-fibular joint has been defined by several studies describing

✉ Delaram Shakoor
delaramshakoor@mail.com

¹ Russell H. Morgan Department of Radiology and Radiological Sciences, Johns Hopkins University, 601 North Caroline Street, Baltimore, MD, USA

² Department of Orthopedic Surgery, Johns Hopkins University, Baltimore, MD, USA

³ Department of Biomedical Engineering, Johns Hopkins University, Baltimore, MD, USA

⁴ Department of Orthopedic Surgery, MedStar Union Memorial Hospital, Baltimore, MD, USA

varying measurements using CT examinations [2, 3, 5, 6, 8–20]. However, most of these studies have been performed on cadavers and almost all of them have utilized conventional CT under nonweight-bearing (NWB) conditions. The advent of dedicated cone-beam CT (CBCT) has allowed evaluation of the lower extremity under physiological WB conditions [21–23]. Previous studies have suggested that this modality might provide a better assessment of lower extremity-related pathological conditions, compared with conventional CT examination, as it may allow detection of subtle injuries that may be missed on NWB CT scan [24, 25]. Few studies have evaluated the tibio-fibular relationship at the level of syndesmosis, under physiological WB condition [2, 3, 24, 26, 27]; however, it is still unclear how the syndesmotic-related measurements change under WB conditions in asymptomatic, uninjured ankles [3, 6, 8, 9, 12–16, 18–20]. To properly assess the influence of a WB load in the syndesmotic joint of post-traumatic ankles, expected changes in WB of syndesmotic measurements in normal ankles should be known [3]. In this study, using cone beam CT examinations of asymptomatic uninjured ankles, we evaluated the influence of WB load in the values of previously defined syndesmotic measurements.

Materials and methods

Patient population

This prospective study was a Health Insurance Portability and Accountability Act (HIPAA)-compliant and Institutional Review Board (IRB)-approved study. Informed consent was obtained from each patient to participate in the study. Between March 2017 and July 2018, both WB and NWB CBCT examinations were performed in 42 patients with a previous ankle fracture, 12 weeks following the injury. The ankle fracture was defined by the referring orthopedic surgeon at the first clinic visit of patients according to the mechanism of injury, the findings of physical examination, and X-ray studies. We included patients with high ankle fractures, including lateral malleolar fracture (Weber B, Weber C), bimalleolar and trimalleolar fractures, which were described to be associated with a high rate of syndesmotic injuries [28]. In 31 patients, CBCT was also obtained from the asymptomatic contralateral ankles. The contralateral ankles were scanned for comparison and to assist in the detection of subtle diastasis in the injured ankles, these ankles were examined by the referring physician to exclude abnormality. For the purposes of this study, only asymptomatic contralateral ankles were included. The medical records and radiographic studies of these 31 patients were reviewed to identify malalignment of the lower leg, previous ankle injuries or surgeries, and the presence of osteoarthritis changes in the contralateral, asymptomatic ankles. The radiographic studies of asymptomatic contralateral ankles were

evaluated by a musculoskeletal radiologist with 8 years of clinical experience to determine the presence of overuse injury and degenerative changes in the tibio-talar and tibio-fibular joints suggestive of osteoarthritis. Three ankles had previous sprains and one ankle had radiographic findings suggestive of ankle osteoarthritis; thus, these four ankles were excluded. Finally, 27 asymptomatic ankles with normal radiographs (10 left ankles and 17 right ankles) of 17 women and 10 men with a mean age of 46.0 ± 17.3 years and a mean BMI of 31.20 ± 7.5 were included in the study.

Cone-beam CT acquisition

All CBCT studies were performed using a cone-beam CT extremity scanner (Research scanner, 2nd generation; Carestream Health, Rochester, NY, USA). Two consecutive CBCTs were performed on the asymptomatic ankles of study subjects:

1. NWB scan was performed while the patient was sitting, with their knee in extension, their ankle in neutral position, and their foot placed over a foam surface in the CBCT gantry
2. WB scan was performed with the patient standing with their feet approximately at shoulder width, distributing the body weight evenly between their lower extremities

The nominal imaging protocol was determined according to previous technical assessment, using 90 kVp and 72 mAs for all scans [29]. Image annotation was removed and each scan was assigned a number. All CBCT imaging data were reconstructed employing a “bone” algorithm, providing images with 0.26-mm isotropic voxels.

Measurement procedure using JMAT software

Measurements were obtained in DICOM-compatible JMAT software [30], developed in-house using Insight tool kit (ITK) libraries. JMAT implements a database of anatomical metrics (as defined below), prescribed in terms of geometric measurements (angles, distances) on user-selected anatomical landmarks. The reader is presented with a multi-planar rendering of CBCT image data to select the landmarks, from which the software automatically computes the measurements (Fig. 1). Landmarks that are common to multiple measurements are re-used between those measurements [30].

Following brief training in the use of JMAT, two independent observers (a board-certified foot and ankle orthopedic surgeon and a post-doctoral radiology fellow with 1 year of clinical experience in the interpretation of musculoskeletal imaging) performed the measurements.

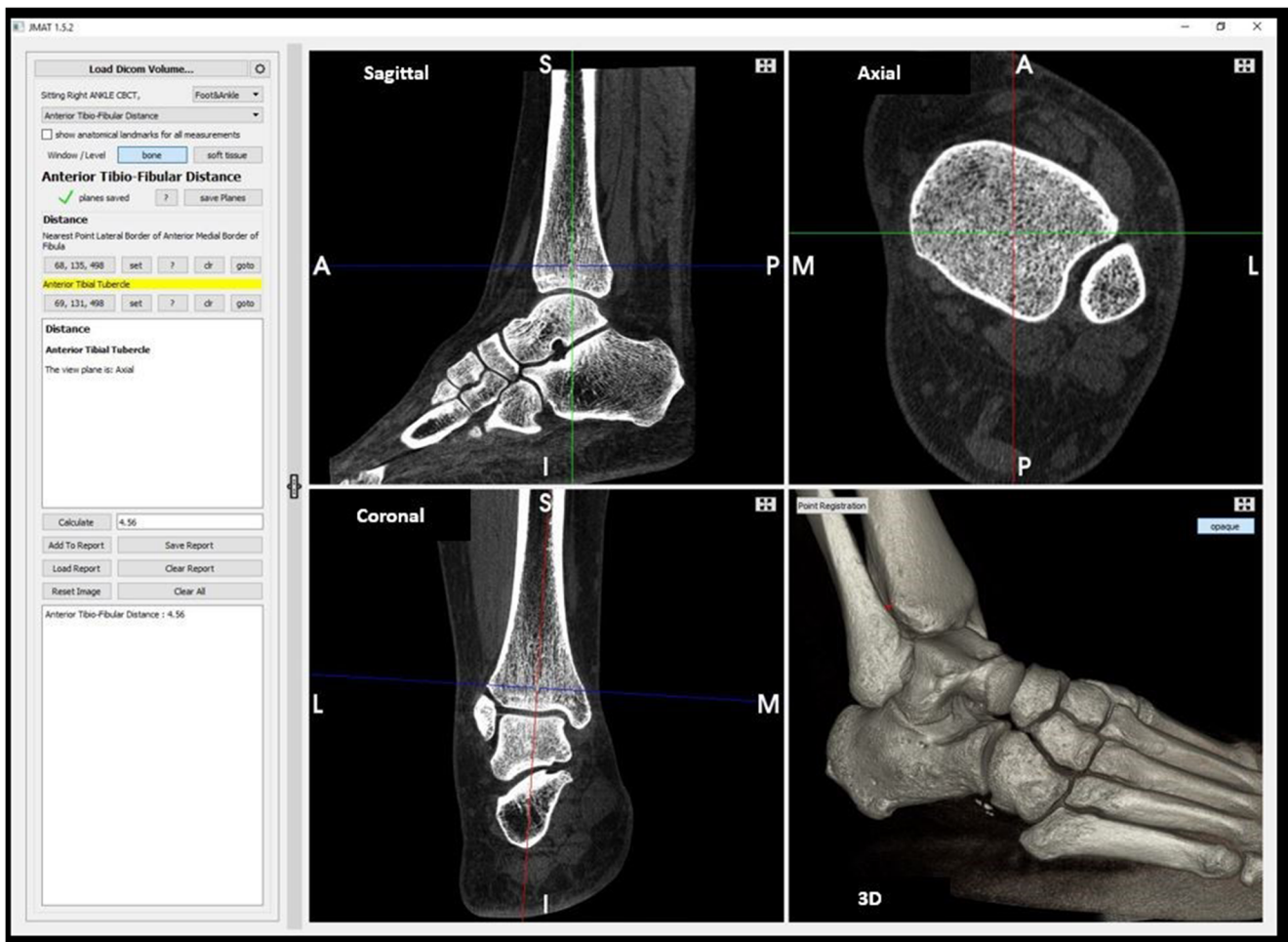


Fig. 1 Determining the first imaging plane (10 mm above the tibial plafond). First, in sagittal and coronal views, vertical planes parallel to the tibial axis are selected. Then, the horizontal plane parallel to the tibial

plafond is selected. Finally, the software automatically moves the selected plane to 10 mm above the pre-determined plane and on axial view the desired plane is obtained

Measurements

Following a comprehensive and systematic literature search, we selected 12 measurements to implement in this project. We attempted to evaluate the syndesmotic measurements in two distinct axial planes:

1. 10 mm above the tibial plafond
2. 5 mm below the talar dome

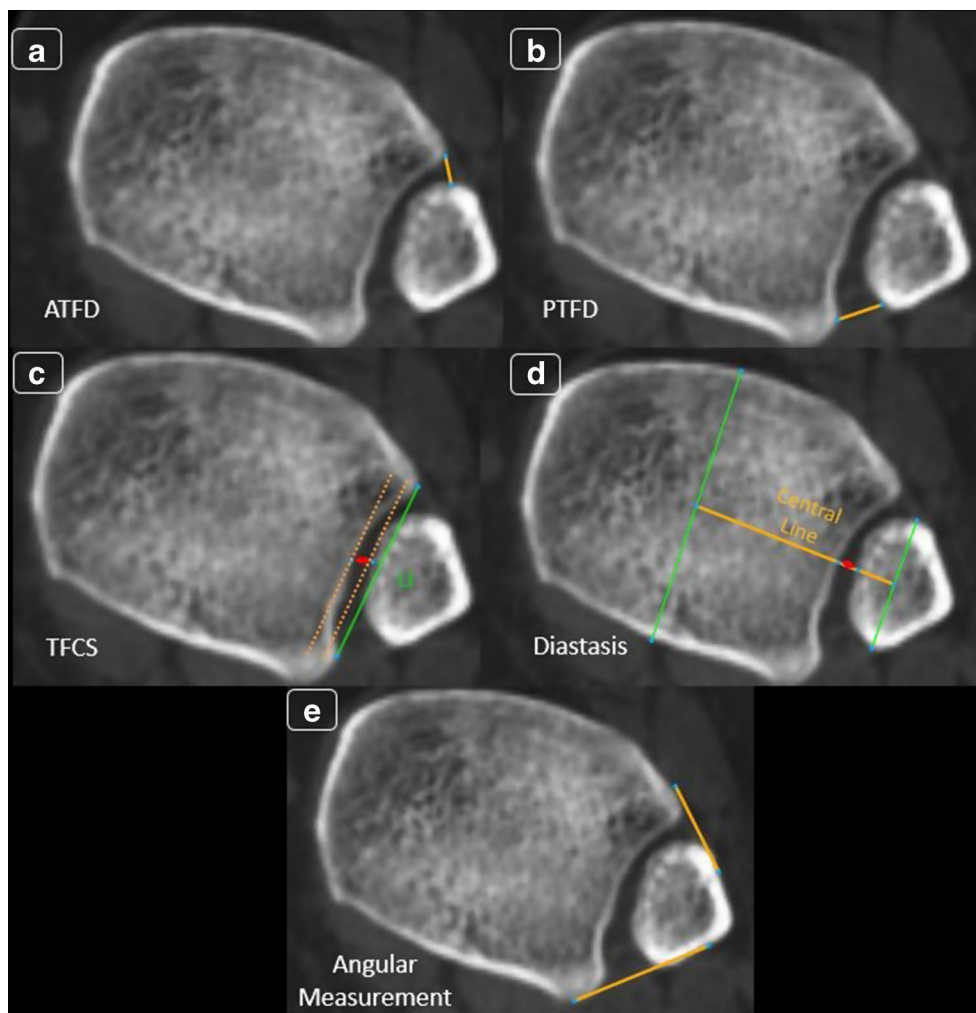
All measurements were defined by different software algorithms, described as follows:

1. Axial plane 1: 10 mm above the tibial plafond. To obtain this imaging plane, the observer selected the plane at the level of the subchondral bone of the tibial plafond and the software automatically moved the selected plane 10 mm above the tibial plafond. At this level, ten measurements, which assessed the diastasis between the tibia and fibula

in addition to the rotation and antero-lateral translation of the fibula in the incisura, were obtained (Fig. 1).

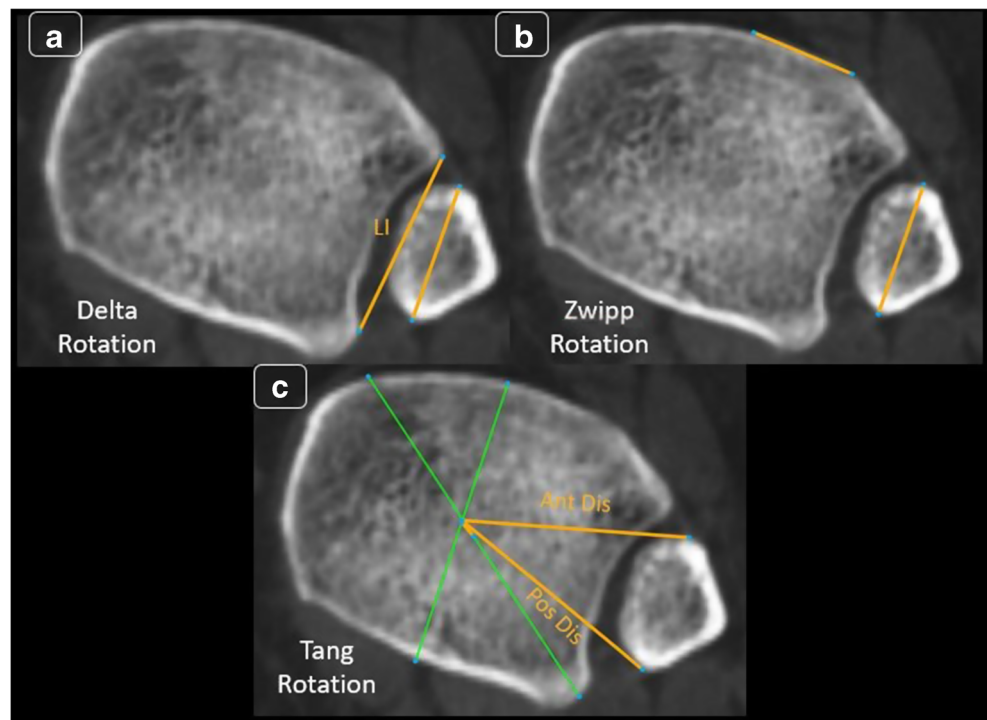
- a) Diastasis between the tibia and fibula:
 - i. Anterior and posterior tibio-fibular distance: As described by Gardner et al. [8] and Elgafy et al. [12], we defined the anterior tibio-fibular distance (ATFD) as the closest distance between the tip of the anterior tibial tubercle and the nearest point on the anterior border of the fibula (Fig. 2a). The posterior tibio-fibular distance (PTFD) was obtained by measuring the distance between the tip of the posterior tibial tubercle and the nearest point on the medial border of the fibula (Fig. 2b).
 - ii. Tibio-fibular clear space: As described by Lepojärvi et al., we first established the tibial incisura length line (LI) by drawing a line between the tips of the anterior and posterior tibial tubercles.

Fig. 2 a–e Measurements evaluating the diastasis between the tibia and fibula at 10 mm above the tibial plafond. *ATFD* anterior tibio-fibular distance, *PTFD* posterior tibio-fibular distance, *TFCS* tibio-fibular clear space, *LI* tibial incisura length line



- Then, parallel to the LI line, we drew two tangential lines at the deepest point of the incisura and the other at the medial border of the fibula. The distance between these two lines was established as the tibio-fibular clear space (TFCS; Fig. 2c).
- iii. Diastasis: As described by Prior et al. [16], the center points of the tibia and fibula were established by determining the center of the lines connecting the anterior and posterior borders of each bone. Then, the centers of these two bones were connected by the central line. Diastasis was obtained by measuring the distance between the medial cortex of the fibula and the lateral cortex of the tibia along the central line (Fig. 2d).
 - iv. Angular measurement: As described by Malhotra et al. [5], the angle created between two tangential lines over the anterior and posterior borders of the tibia and lateral malleolus was determined as the angular measurement (Fig. 2e).
- b) Rotation of the fibula relative to the incisura fibularis:
 - i. Δ_{FIB} : The Δ_{FIB} measurement, as described by Dikos et al. [9], was the angle created between the LI and the line across the anterior and posterior tubercles of the fibula (Fig. 3a).
 - ii. Zwipp rotation: As described by Zwipp in 1994 [19] and later by Vasarhelyi et al. in 2006 [18], the Zwipp rotation is the angle created by the line across the anterior and posterior tubercles of the fibula and the tangential line to the anterior-most point of the tibia (Fig. 3b).
 - iii. Tang rotation: First, for this measurement, multiple bisecting lines were drawn over tibial surface to determine the summation of these lines as the center of the tibia. Then, the distances between this center point and the anterior and posterior points of the fibula were measured. The Tang rotation was determined as the ratio of the anterior distance over the posterior distance (Fig. 3c) [15].

Fig. 3 Measurements evaluating the rotation of the fibula relative to the incisura at 10 mm above the tibial plafond. *LI* tibial incisura length line, *Ant Dis* anterior distance, *Pos Dis* posterior distance



c) Translation of the fibula relative to the incisura:

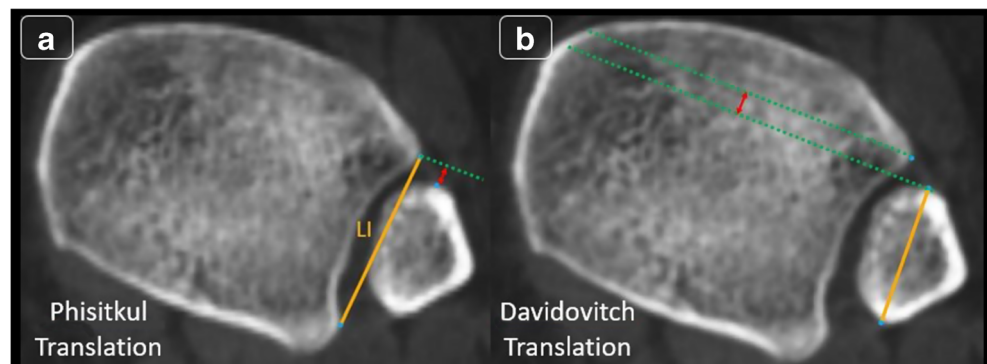
- i. Phisitkul translation: For this measurement, a perpendicular line to the LI was drawn at the level of the anterior tibial tubercle. Then, the distance from this perpendicular line to the anterior-most point of the fibula was established as the Phisitkul translation [13]. If the fibula was located posterior to the perpendicular line, the measurement was positive and if the fibula was located anterior to the perpendicular line, the measurement value was considered to be negative (Fig. 4a).
- ii. Davidovitch translation: First, for this measurement, the line connecting the widest portion of the fibula from anterior to posterior was drawn. Then, a perpendicular line to this connecting

line was drawn at the anterior-most point of the fibula. Then, a parallel line to the last line was drawn at the anterior tibial tubercle. The distance between these two parallel lines was established as the Davidovitch translation (Fig. 4b) [14].

2. Axial plane 2: 5 mm below the talar dome. To obtain this plane, the observer selected the plane at the level of the subchondral bone of the talar dome. Then, the software automatically moved the selected plane 5 mm below the talar dome. At this level, we performed two measurements evaluating the anatomy of the ankle mortise (Fig. 5).

- a) Lateral clear space: The shortest distance between the lateral malleolus and talus was determined as the lateral clear space (LCS; Fig. 6a) [31].

Fig. 4 Measurements evaluating the translation of the fibula relative to the incisura at 10 mm above the tibial plafond. *LI* tibial incisura length line



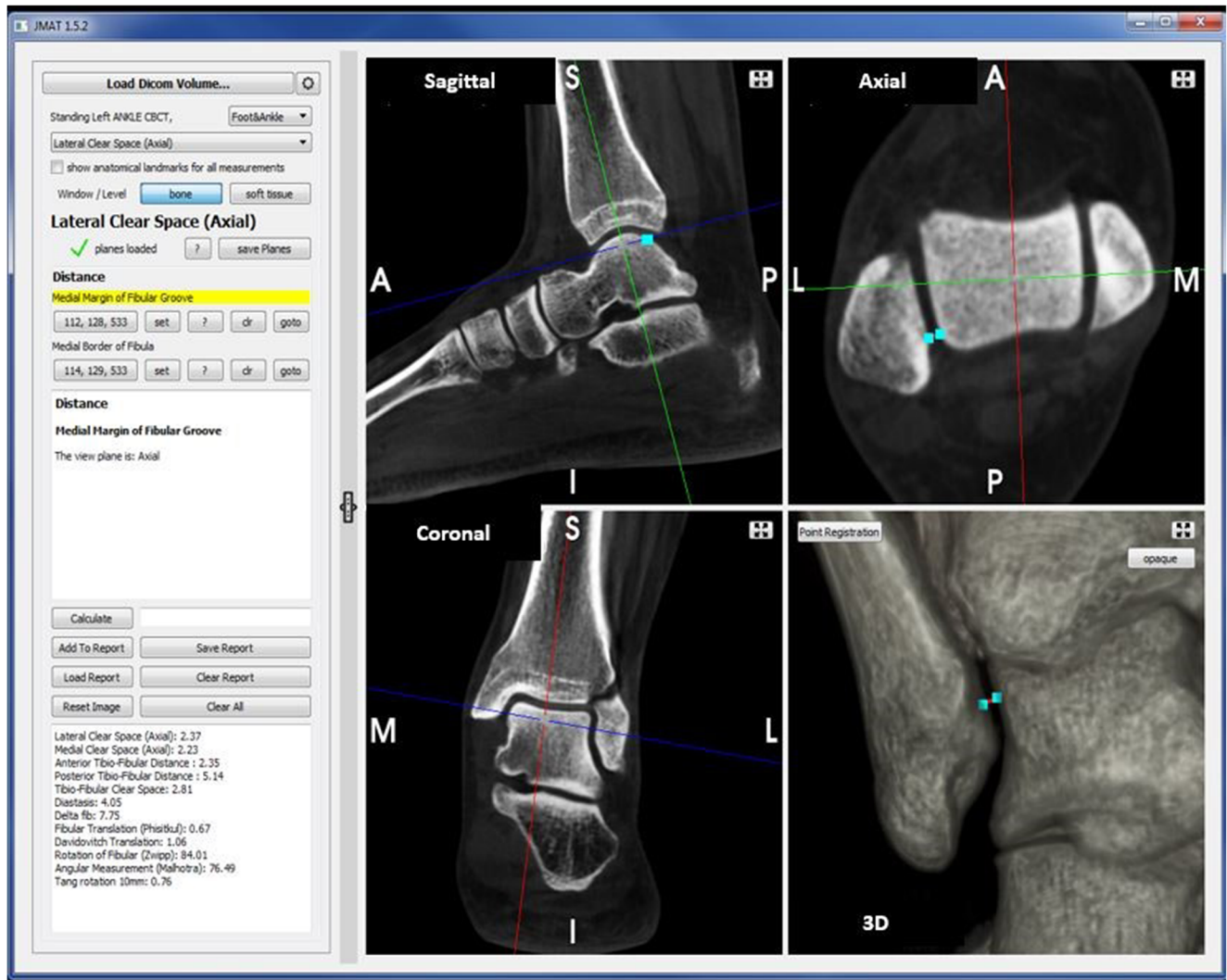


Fig. 5 Determining the second imaging plane (5 mm below the talar dome). First, in the sagittal and coronal views, vertical planes parallel to the tibial axis are selected. Then, the horizontal plane parallel to the talar

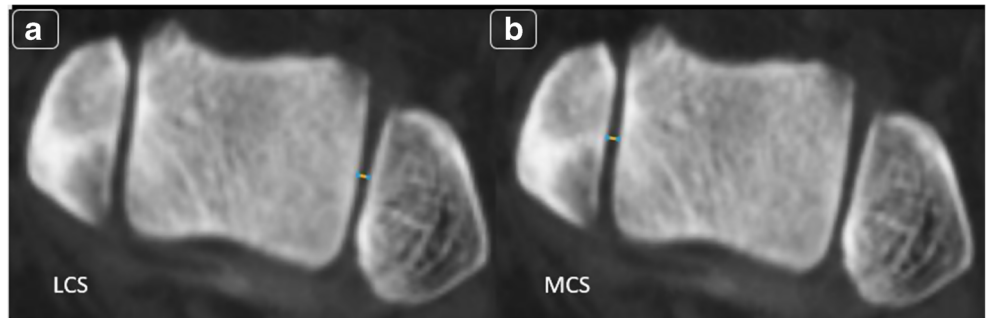
dome is selected. Finally, the software automatically moves the selected plane to 5 mm below the pre-determined plane and in the axial view, the desired plane is obtained

- b) Medial clear space: The shortest distance between the medial malleolus and talus was determined as the medial clear space (MCS; Fig. 6b) [31].

Statistical analysis

To assess for the normality of the data distribution of each measurement, the Shapiro–Wilk test was used. Intra-class

Fig. 6 Measurements 5 mm below the talar dome evaluating the lateral clear space (LCS) and the medial clear space (MCS)



correlation coefficient (ICC) was used to evaluate the inter-observer reliability between two readers (two-way random model for absolute agreement) [32]. ICC values higher than 0.74 were considered to show excellent correlation between readers, ICC values between 0.6 and 0.74 indicated good correlation, ICC values between 0.4 and 0.6 were regarded as fair correlation, and values lower than 0.4 were considered a poor correlation [22, 33, 34]. WB and NWB measurements were compared employing paired Students *t* tests or Wilcoxon rank-sum tests, according to the normality of the distribution of data. We also investigated whether there were any differences between men and women using similar statistics. To compensate for our relatively small sample size, bootstrapping or Monte Carlo simulation with 10,000 samples was applied to calculate robust estimates of confidence intervals and *p*-values for 99% uncertainty levels. Benjamin–Hochberg (BH) corrections was used to calculate multiple testing-adjusted *p* values. PASW (V.20; SPSS, Chicago, IL, USA) and STATA software (version 14; StataCorp, College Station, TX, USA) were used to perform the analysis.

Results

We observed that the measurements employed had statistically significantly good inter-observer agreement between two observers in both WB (mean ICC: 0.73; range: 0.62, 0.9, *p* < 0.05) and NWB images (mean ICC: 0.68; range: 0.44, 0.82, *p* < 0.05; Table 1). Mean values along with their 95% confidence interval (95% CI), and the median and range of our measurements were described in Table 2. All values of

measurements except for those of Tang rotation, Phisitkul translation, and MCS had a normal distribution of data.

Regarding measurements evaluating diastasis between the tibia and fibula, including ATFD, PTFD, TFCS, diastasis, and angular measurement, we did not observe any statistically significant changes when the WB condition was applied (*p* > 0.05; Table 3). Similarly, mean values of fibular rotation and translation of the fibula relative to the incisura were not significantly different between WB and NWB images (*p* > 0.05). When assessing the position of the talus in the ankle mortise, we observed that mean values of the MCS were significantly lower on WB images compared with NWB images (mean of difference: −0.3, 95% CI: −0.47, −0.12, *p* = 0.01). Although mean values of the LCS were lower in the WB position, the difference was not statistically significantly different (mean of difference: −0.09, 95% CI: −0.26, 0.06; *p* = 0.5; Table 3). Gender showed no influence on any of the measurements obtained, for both WB and NWB images (*p* > 0.05; Table 4). Also, diastasis and delta rotation, which had excellent inter-observer agreement on both WB and NWB images, were compared in Fig. 7.

Discussion

The present study is the first attempt to assess the effect of weight-bearing on syndesmotomic measurements in a population of asymptomatic uninjured ankles with a normal plain radiograph. Our results indicate that the position of the fibula in the incisura remains unchanged when the WB condition is applied. Our findings confirm those of previous studies, which

Table 1 Level of agreement between two observers for all measurements

	Weight-bearing	95% confidence interval	Level of agreement	Nonweight-bearing	95% confidence interval	Level of agreement
ATFD	0.62	0.18, 0.82	Good	0.75	0.34, 0.89	Excellent
PTFD	0.68	0.25, 0.86	Good	0.73	0.17, 0.91	Good
TFCS	0.83	0.01, 0.94	Excellent	0.7	0.35, 0.86	Good
Diastasis	0.90	0.56, 0.96	Excellent	0.82	0.35, 0.93	Excellent
Angular measurement	0.60	0.11, 0.81	Good	0.77	0.49, 0.89	Excellent
Delta rotation	0.76	0.42, 0.89	Excellent	0.82	0.62, 0.92	Excellent
Zwipp rotation	0.88	0.74, 0.94	Excellent	0.74	0.42, 0.88	Good
Tang rotation	0.70	0.32, 0.86	Good	0.44	0.01, 0.73	Fair
Phisitkul translation	0.60	0.16, 0.81	Good	0.68	0.32, 0.85	Good
Davidovitch translation	0.74	0.38, 0.88	Good	0.50	0.02, 0.76	Fair
LCS	0.80	0.53, 0.91	Excellent	0.72	0.36, 0.87	Good
MCS	0.65	0.24, 0.84	Good	0.49	0.01, 0.76	Fair

ICC: 0.75–1 excellent; 0.6–0.74 good; 0.4–0.6 fair; 0.4 poor

ATFD anterior tibio-fibular distance, PTFD posterior tibio-fibular distance, TFCS tibio-fibular clear space, LCS lateral clear space, MCS medial clear space

Table 2 Descriptive data showing mean, median, and range of measurements

	Weight-bearing			Nonweight-bearing		
	Mean (95% CI)	Median (IQR)	Range	Mean (95% CI)	Median (IQR)	Range
Diastasis between the tibia and fibula						
ATFD	3.69 (3.3, 3.9)	3.54 (1.1)	2.24, 5.17	3.68 (3.3, 4)	3.57 (1.3)	2.20, 5.22
PTFD	5.71 (5.3, 6.1)	5.66 (1.68)	3.94, 8.67	5.66 (5.1, 6.2)	5.53 (1.85)	3.67, 9.24
TFCS	3.29 (2.9, 3.7)	3.32 (1.52)	1.42, 4.79	3.30 (2.8, 3.8)	3.43 (1.90)	0.99, 6.51
Diastasis	3.16 (2.7, 3.5)	3.25 (1.62)	1.2, 5.53	3.03 (2.6, 3.4)	2.82 (1.73)	1.05, 4.69
Angular measurement	71.83 (69.1, 74.5)	72.35 (8.2)	58.33, 84.82	71.68 (68.9, 74.4)	71.22 (8.77)	61.42, 85.43
Fibular rotation						
Delta rotation	10.75 (8.7, 12.8)	10.88 (8.26)	1.82, 24.07	12.32 (10.2, 14.4)	12.62 (7.84)	2.04, 25.03
Zwipp rotation	92.76 (89.0, 96.5)	92.41 (14.88)	72.82, 109.12	93.53 (90.5, 96.6)	95.12 (12.13)	77.85, 111.48
Tang rotation	0.85 (0.83, 0.87)	0.84 (0.05)	0.77, 0.99	0.85 (0.83, 0.87)	0.84 (0.07)	0.77, 0.93
Fibular translation						
Phisitkul translation	1.66 (1.3, 2.0)	1.85 (1.17)	−0.65–3.6	1.39 (0.8, 1.9)	1.93 (1.8)	−1.83, 3.02
Davidovitch translation	2.26 (1.9, 2.6)	2.30 (1.3)	0.53, 4.36	2.51 (2.2, 2.9)	2.65 (1.24)	1.04, 4.43
Ankle mortise						
LCS	1.88 (1.7, 2)	1.85 (0.64)	1, 2.77	1.97 (1.8, 2.1)	1.82 (0.6)	1.2, 2.79
MCS	1.74 (1.6, 1.9)	1.78 (0.54)	1.25, 2.51	2.02 (1.8, 2.2)	1.85 (0.8)	1.29, 3.85

reported that in the presence of an intact syndesmosis, the tibio-fibular relationship remains stable [35, 36]. Beumer et al. performed a radiostereometric study on ten cadaveric specimens and assessed the tibio-fibular relation when a load of 750 N was applied. They reported that when a load was applied, the mean difference in lateral–medial displacement was −0.24 mm (95% CI: −0.63, 0.14), which is comparable with our results on measurements evaluating the diastasis between the tibia and fibula, particularly the TFCS [35]. Also,

the authors reported that the mean difference in anterior–posterior displacement was 0.13 mm (95% CI: −0.56, 0.81), which is comparable with our measurements evaluating the translation of the fibula to the incisura [35]. Our results are also consistent with those of previous studies that showed that syndesmotomic measurements were not significantly different in men and women, despite the differences in the ankle joint dimensions and shape and depth of the incisura [9, 37]. As described in a previous study by Dikos et al., we also observed

Table 3 Mean difference values of measurements on weight-bearing and nonweight-bearing images

	Mean difference between WB and NWB	95% confidence interval	<i>p</i> value	BH correction
Diastasis between the tibia and fibula				
ATFD	0.007	−0.26, 0.27	0.9	0.96
PTFD	0.056	−0.30, 0.41	0.74	0.88
TFCS	−0.005	−0.26, 0.25	0.96	0.96
Diastasis	0.133	−0.0001, 0.26	0.05	0.19
Angular measurement	0.15	−1.54, 1.84	0.8	0.8
Fibular rotation				
Delta rotation	−1.57	−3.32, 0.17	0.07	0.1
Zwipp rotation	−0.76	−3.10, 1.56	0.50	0.6
Tang rotation	0.004	−0.009, 0.01	0.51	0.6
Fibular translation				
Phisitkul translation	0.26	−0.12, 0.65	0.16	0.3
Davidovitch translation	−0.25	−0.54, 0.03	0.082	0.19
Ankle mortise				
LCS	−0.092	−0.24, 0.05	0.2	0.3
MCS	−0.27	−0.44, −0.11	<0.001	0.01

Bold data is the only measurement that was significantly different between two scans

Table 4 Comparison between men and women of the measurements obtained

	Weight-bearing			Nonweight-bearing		
	Median (IQR) male	Median (IQR) female	<i>p</i> value after BH Correction	Median (IQR) male	Median (IQR) female	<i>p</i> value after BH correction
Diastasis between the tibia and fibula						
ATFD	3.58 (1.57)	3.54 (1.08)	0.7	3.45 (1.25)	3.78 (1.35)	0.6
PTFD	6.24 (2.27)	5.6 (1.14)	0.6	5.50 (1.75)	5.53 (1.92)	0.7
TFCFS	3.31 (1.92)	3.41 (1.55)	0.8	3.26 (1.91)	3.53 (1.89)	0.8
Diastasis	3.35 (1.78)	3.11 (1.28)	0.6	3.06 (2.20)	2.82 (1.45)	0.8
Angular measurement	69.52 (8.6)	72.40 (11.77)	0.6	70.95 (10.27)	71.42 (11.74)	0.9
Fibular rotation						
Delta rotation	8.65 (9.14)	12.21 (7.11)	0.4	11.83 (10.76)	12.62 (5.29)	0.8
Zwipp rotation	94.35 (16.62)	90.67 (16.78)	0.5	93.68 (12.92)	95.49 (10.86)	0.6
Tang rotation	0.88 (0.05)	0.84 (0.03)	0.1	0.88 (0.11)	0.84 (0.05)	0.4
Fibular translation						
Phisitkul translation	1.34 (0.96)	2.03 (1.05)	0.2	0.87 (3.51)	1.93 (1.03)	0.4
Davidovitch translation	1.99 (1.53)	2.62 (1.2)	0.2	1.82 (1.43)	2.67 (1.11)	0.4
Ankle mortise						
LCS	1.90 (0.73)	1.79 (0.68)	0.2	2.16 (0.83)	1.77 (0.38)	0.1
MCS	1.95 (0.45)	1.55 (0.59)	0.2	2.31 (0.60)	1.67 (0.52)	0.2

that the diastasis and delta rotation in male and female patients were not statistically significantly different (Fig. 7) [9].

We observed that during the WB condition, the ankle mortise becomes slightly tighter, as demonstrated by the significant decrease in the MCS. However, the MCS measurements are highly variable and very subjective [38]. In a previous study, the dynamics of the tibio-talar joint was explored under the WB condition [38]. Lepojärvi et al. observed that when the

ankle was internally/externally rotated, the talus rotated without a significant change in the MCS. However, the authors did not compare WB and NWB measurements. It could be hypothesized that, under the WB condition, the talus might rotate and, considering its irregular shape with the wider anterior aspect of the talar dome, it might get closer to the medial malleolus, decreasing the MCS. However, it should be noted that we did not investigate the dynamics of a normal tibio-talar

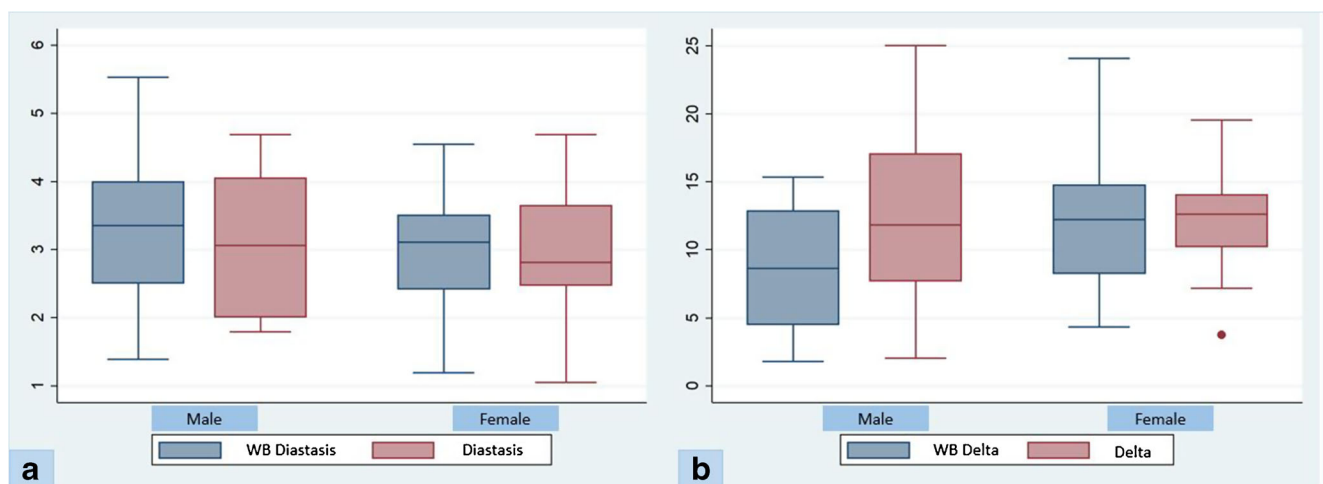


Fig. 7 Comparison of measurements in men and women. Weight-bearing measurements were shown with blue boxes and nonweight-bearing measurements were shown with red boxes. **a** Diastasis between the tibia

and fibula at 10 mm above the tibial plafond. **b** Delta rotation at 10 mm above the tibial plafond

joint and further studies are warranted to define the normal anatomy of the tibio-talar joint and assess its change when the WB condition is applied.

Our findings are inconsistent with those of a recently published study by Malhotra et al. [2], which compared the syndesmotic measurements of WB CBCT and a conventional NWB CT. They reported that during WB, the fibula translates posteriorly and laterally along with external rotation [2]. Several differences in the design, execution, and the measurements may have led to this discrepancy. First, our study subjects included asymptomatic uninjured ankles, whereas in the study by Malhotra et al., symptomatic ankles were included. Although they excluded those who had syndesmotic-related symptoms and pathological conditions, they included patients with ankle osteoarthritis and talar osteochondral lesions and they did not provide any data on the etiologies of these pathological conditions. It has been well established that most cases of ankle osteoarthritis are post-traumatic [39, 40] and 70–98% of talar osteochondral lesions are reported to be associated with previous trauma [41]. Missed syndesmosis injuries may also have contributed to increased tibio-talar contact stress and subsequent degenerative changes [1, 42]. Thus, the inclusion of patients with likely post-traumatic pathological conditions may have altered their results. Second, the same scanner was not used to perform their WB and NWB CT scans and their WB and NWB scans were separated by an interval of 1–3 years, which could have had an impact on their measurements. Third, the rotation of the ankle was not controlled in the study by Malhotra et al. as it was in ours by placing the patient in a neutral position in both NWB and WB modes. The degree of plantarflexion/dorsiflexion of the ankle and its associated rotation were described to have an impact on the position of the fibula [3]. Therefore, to assess only the effect of WB on the syndesmotic measurements, the impact of ankle rotation and dorsiflexion should be minimized. In our study, we used the same scanner to perform consecutive scans with essentially no interval between WB and NWB scans obtained in sequence. Also, during the NWB scan, the ankles were put on dedicated foam to minimize the amount of ankle rotation and dorsiflexion during the scan. Thus, it could be assumed that the true effect of weight was evaluated without the related bias of ankle rotation or dorsiflexion. Finally, we performed a comprehensive review of the literature and selected the most frequent measurements in two standardized axial planes with respect to the tibio-talar joint. As the accuracy of each measurement for detecting syndesmotic measurements has not been reported and no CT-based gold standard assessment of syndesmotic injuries exists, we implemented several measurements to comprehensively assess the effect of WB on normal the tibio-fibular relationship. In the study by Malhotra et al., they implemented the measurements in one plane, suggested by one study [10], which was entirely distinct from the measurements that we employed.

We acknowledge that our study had several limitations. First, we attempted to recruit asymptomatic ankles with intact syndesmosis by including those with normal examination and no previous surgeries or ankle injuries. Thus, we did not have arthroscopic findings confirming the integrity of syndesmosis in our study subjects. Considering the high prevalence of ankle injuries, our sample size consisting of asymptomatic uninjured ankles was relatively small. Second, the CBCT slices were approximately 0.3 mm thick and thus smaller changes may have been difficult to detect. Therefore, it may be plausible that our study was underpowered to detect the difference when the WB condition was applied and our data may not be generalizable to the normal population. The variability that was detected in each measurement in our study may be used to calculate the power required for a study that may detect statistically significant differences generalizable to the normal population. Third, we used semi-automatic software to minimize the element of subjectivity and improve workflow. However, the software computed the measurements from anatomical landmarks that were selected by the readers, and thus, the element of subjectivity was not completely eliminated. Besides, we did not assess the impact of this software on the workflow and reading time. Further studies are required to investigate how much this software will improve workflow in clinical practice. Despite observing good agreement between our readers, only one of our readers was a board-certified foot and ankle surgeon. However, it should be noted that before performing the measurements, our readers underwent a training period, supervised by a musculoskeletal radiologist with 8 years of clinical experience.

In conclusion, the findings of our study have shown that previously defined syndesmotic measurements can be reliably performed on WB images. Except for the MCS, no significant differences were found in syndesmotic measurements when comparing NWB and WB conditions. This implies that under a physiological load, the relationship between the distal tibia and fibula remains unchanged in the presence of an intact syndesmosis. Thus, any difference between weight-bearing and nonweight-bearing measurements could suggest an underlying pathological condition in the ankle joint. Further studies with larger sample sizes are warranted to robustly address this issue.

Compliance with ethical standards

Conflicts of interest Delarm Shakoor, Michael Brehler, Cesar de Cesar Netto, Babar Shafiq, Jakrapong Orapin, Gauarav K Thawait declared that they have no conflicts of interest.

Greg M Osgood received research support from Carestream Health.

Wojciech B Zbijewski received a research grant from Carestream Health.

Lew C Schon received research grants from Zimmer, Wright Medical, Smith-Nephew, Spine-Smith/Celing Bioscience, Carestream Health, and received research support from Arthrex, DJO, and DARCO.

Shadpour Demehri received research support from the General Electric company and Carestream Health, and is also a consultant for Toshiba Corporation.

References

- Ramsey PL, Hamilton W. Changes in tibiotalar area of contact caused by lateral talar shift. *J Bone Joint Surg Am.* 1976;58(3):356–7.
- Malhotra KWM, Cullen N, Singh D, Goldberg AJ. The effects of weight bearing on the distal tibiofibular syndesmosis: a study comparing weight bearing-CT with conventional CT. *Foot Ankle Surg.* 2018. <https://doi.org/10.1016/j.fas.2018.03.006>.
- Lepojärvi S, Niinimäki J, Pakarinen H, Leskelä HV. Rotational dynamics of the normal distal tibiofibular joint with weight-bearing computed tomography. *Foot Ankle Int.* 2016;37(6):627–35.
- Rammelt S, Obruba P. An update on the evaluation and treatment of syndesmotic injuries. *Eur J Trauma Emerg Surg.* 2015;41(6):601–14.
- Malhotra G, Cameron J, Toolan BC. Diagnosing chronic diastasis of the syndesmosis: a novel measurement using computed tomography. *Foot Ankle Int.* 2014;35(5):483–8.
- Ahn TK, Choi SM, Kim JY, Lee WC. Isolated syndesmosis diastasis: computed tomography scan assessment with arthroscopic correlation. *Arthroscopy.* 2017;33(4):828–34.
- Espinosa N, Smerek JP, Myerson MS. Acute and chronic syndesmosis injuries: pathomechanisms, diagnosis and management. *Foot Ankle Clin.* 2006;11(3):639–57.
- Gardner MJ, Demetrakopoulos D, Briggs SM, Helfet DL, Lorich DG. Malreduction of the tibiofibular syndesmosis in ankle fractures. *Foot Ankle Int.* 2006;27(10):788–92.
- Dikos GD, Heisler J, Choplin RH, Weber TG. Normal tibiofibular relationships at the syndesmosis on axial CT imaging. *J Orthop Trauma.* 2012;26(7):433–8.
- Nault ML, Hebert-Davies J, Laflamme GY, Leduc S. CT scan assessment of the syndesmosis: a new reproducible method. *J Orthop Trauma.* 2013;27(11):638–41.
- Ebraheim NA, Lu J, Yang H, Mekhail AO, Yeasting RA. Radiographic and CT evaluation of tibiofibular syndesmosis diastasis: a cadaver study. *Foot Ankle Int.* 1997;18(11):693–8.
- Elgafy H, Semaan HB, Blessinger B, Wassef A, Ebraheim NA. Computed tomography of normal distal tibiofibular syndesmosis. *Skeletal Radiol.* 2010;39(6):559–64.
- Phisitkul P, Ebinger T, Goetz J, Vaseenon T, Marsh JL. Forceps reduction of the syndesmosis in rotational ankle fractures: a cadaveric study. *J Bone Joint Surg Am.* 2012;94(24):2256–61.
- Davidovitch RI, Weil Y, Karia R, Forman J, Looze C, Liebergall M, et al. Intraoperative syndesmotic reduction: three-dimensional versus standard fluoroscopic imaging. *J Bone Joint Surg Am.* 2013;95(20):1838–43.
- Tang CW, Roidis N, Vaishnav S, Patel A, Thordarson DB. Position of the distal fibular fragment in pronation and supination ankle fractures: a CT evaluation. *Foot Ankle Int.* 2003;24(7):561–6.
- Prior CP, Widnall JC, Rehman AK, Weller DM, Wood EV. A simplified, validated protocol for measuring fibular reduction on ankle CT. *Foot Ankle Surg.* 2017;23(1):53–6.
- Mukhopadhyay S, Metcalfe A, Guha AR, Mohanty K, Hemmati S, Lyons K, et al. Malreduction of syndesmosis—are we considering the anatomical variation? *Injury.* 2011;42(10):1073–6.
- Vasarhelyi A, Lubitz J, Gierer P, Gradl G, Rosler K, Hopfenmuller W, et al. Detection of fibular torsional deformities after surgery for ankle fractures with a novel CT method. *Foot Ankle Int.* 2006;27(12):1115–21.
- Zwipp H. *Chirurgie des Fusses.* Vienna: Springer; 1994.
- Knops SP, Kohn MA, Hansen EN, Matityahu A, Marmor M. Rotational malreduction of the syndesmosis: reliability and accuracy of computed tomography measurement methods. *Foot Ankle Int.* 2013;34(10):1403–10.
- De Cesar Netto C, Schon LC, Thawait GK, da Fonseca LF, Chinanuvathana A, Zbijewski WB, et al. Flexible adult acquired flatfoot deformity: comparison between weight-bearing and non-weight-bearing measurements using cone-beam computed tomography. *J Bone Joint Surg Am.* 2017;99(18):e98.
- De Cesar Netto C, Shakoor D, Dein EJ, Zhang H, Thawait GK, Richter M, et al. Influence of investigator experience on reliability of adult acquired flatfoot deformity measurements using weightbearing computed tomography. *Foot Ankle Surg.* 2018. <https://doi.org/10.1016/j.fas.2018.03.001>.
- Osgood GM, Thawait GK, Hafezi-Nejad N, Shakoor D, Shaner A, Yorkston J, et al. Image quality of cone beam computed tomography for evaluation of extremity fractures in the presence of metal hardware: visual grading characteristics analysis. *Br J Radiol.* 2017;90(1073):20160539.
- Marzo JM, Kluczynski MA, Clyde C, Anders MJ, Mutty CE, Ritter CA. Weight bearing cone beam CT scan versus gravity stress radiography for analysis of supination external rotation injuries of the ankle. *Quant Imaging Med Surg.* 2017;7(6):678–84.
- Thawait GK, Demehri S, AlMuhit A, Zbijewski W, Yorkston J, Del Grande F, et al. Extremity cone-beam CT for evaluation of medial tibiofemoral osteoarthritis: initial experience in imaging of the weight-bearing and non-weight-bearing knee. *Eur J Radiol.* 2015;84(12):2564–70.
- Lawlor MC, Kluczynski MA, Marzo JM. Weight-bearing cone-beam CT scan assessment of stability of supination external rotation ankle fractures in a cadaver model. *Foot Ankle Int.* 2018;39(7):850–57.
- Lintz F, de Cesar Netto C, Barg A, Burssens A, Richter M. Weight-bearing cone beam CT scans in the foot and ankle. *EFORT Open Rev.* 2018;3(5):278–86.
- Carr JC 2nd, Werner BC, Yarburo SR. An update on management of syndesmosis injury: a national US database study. *Am J Orthop (Belle Mead NJ).* 2016;45(7):E472–7.
- Carrino JA, Al Muhit A, Zbijewski W, Thawait GK, Stayman JW, Packard N, et al. Dedicated cone-beam CT system for extremity imaging. *Radiology.* 2014;270(3):816–24.
- Brehler M, Thawait G, Shyr W, Ramsay J, Siewerdsen JH, Zbijewski W. Atlas-based automatic measurements of the morphology of the tibiofemoral joint. *Proc SPIE Int Soc Opt Eng.* 2017;10137:101370E.
- Pelton K, Thordarson DB, Barnwell J. Open versus closed treatment of the fibula in Maisonneuve injuries. *Foot Ankle Int.* 2010;31(7):604–8.
- Koo TK, Li MY. A guideline of selecting and reporting intraclass correlation coefficients for reliability research. *J Chiropr Med.* 2016;15(2):155–63.
- Fleiss JL. *Statistical methods for rates and proportions.* New York: Wiley; 1981.
- Ellis SJ, Deyer T, Williams BR, Yu JC, Lehto S, Maderazo A, et al. Assessment of lateral hindfoot pain in acquired flatfoot deformity using weightbearing multiplanar imaging. *Foot Ankle Int.* 2010;31(5):361–71.
- Beumer A, Valstar ER, Garling EH, Niesing R, Ginai AZ, Ranstam J, et al. Effects of ligament sectioning on the kinematics of the distal tibiofibular syndesmosis: a radiostereometric study of 10 cadaveric specimens based on presumed trauma mechanisms with suggestions for treatment. *Acta Orthop.* 2006;77(3):531–40.
- Norkus SA, Floyd RT. The anatomy and mechanisms of syndesmotic ankle sprains. *J Athl Train.* 2001;36(1):68–73.
- Anand Prakash A. Syndesmotic stability: is there a radiological normal?—A systematic review. *Foot Ankle Surg.* 2018;24(3):174–84.
- Lepojärvi S, Niinimäki J, Pakarinen H, Koskela L, Leskelä HV. Rotational dynamics of the talus in a normal tibiotalar joint as

- shown by weight-bearing computed tomography. *J Bone Joint Surg Am.* 2016;98(7):568–75.
39. Buckwalter JA, Saltzman C, Brown T. The impact of osteoarthritis: implications for research. *Clin Orthop Relat Res.* 2004;427:S6–15.
 40. Brown TD, Johnston RC, Saltzman CL, Marsh JL, Buckwalter JA. Posttraumatic osteoarthritis: a first estimate of incidence, prevalence, and burden of disease. *J Orthop Trauma.* 2006;20(10):739–44.
 41. O'Loughlin PF, Heyworth BE, Kennedy JG. Current concepts in the diagnosis and treatment of osteochondral lesions of the ankle. *Am J Sports Med.* 2010;38(2):392–404.
 42. Lloyd J, Elsayed S, Hariharan K, Tanaka H. Revisiting the concept of talar shift in ankle fractures. *Foot Ankle Int.* 2006;27(10):793–6.